Adaptive Control Strategy for the Dynamic Positioning of a Shuttle Tanker During Offloading Operations

Eduardo A. Tannuri
e-mail: eduat@usp.br

Leonardo K. Kubota
e-mail: leonardo.kubota@poli.usp.br

Department of Naval Architecture and Ocean Engineering,
University of São Paulo,
São Paulo, SP,
Brazil

Celso P. Pesce
Department of Mechanical Engineering,
University of São Paulo,
São Paulo, SP,
Brazil
e-mail: ceppesce@usp.br

In deep water oil production, Dynamic positioning systems (DPS) strategy has shown to be an effective alternative to tugboats, in order to control the position of the shuttle tanker during offloading operations from a FPSO (floating production, storage, and offloading system). DPS reduces time, cost, and risks. Commercial DPS systems are usually based on control algorithms which associate Kalman filtering techniques with proportional-derivative (PD) or optimal linear quadratic (LQ) controllers. Since those algorithms are, in general, based on constant gain controllers, performance degradation may be encountered in some situations, as those related to mass variation during the loading operation of the shuttle tanker. The positioning performance of the shuttle changes significantly, as the displacement of the vessel increases by a factor of three. The control parameters are adjusted for one specific draught, making the controller performance to vary. In order to avoid such variability, a human-based periodic adjustment procedure might be cogitated. Instead and much safer, the present work addresses the problem of designing an invariant-performance control algorithm through the use of a robust model-reference adaptive scheme, cascaded with a Kalman filter. Such a strategy has the advantage of preserving the simple structure of the usual PD and LQ controllers, the adaptive algorithm itself being responsible for the on-line correction of the controller gains, thus insuring a steady performance during the whole operation. As the standard formulation of adaptive controllers does not guarantee robustness regarding modeling errors, an extra term was included in the controller to cope with strong environmental disturbances that could affect the overall performance. The controller was developed and tested in a complete mathematical simulator, considering a shuttle tanker operating in Brazilian waters subjected to waves, wind and current. The proposed strategy is shown to be rather practical and effective, compared with the performance of constant gain controllers. [DOI: 10.1115/1.2199559]

Keywords: adaptive control, dynamic positioning system, Kalman filter

Introduction

Dynamic positioning systems (DPS) are defined as a set of components used to keep a floating vessel on a specific position or pre-defined path through the action of propellers. DPS include position and heading measurement systems, a set of control algorithms, and propellers. Several offshore operations are carried out using DPS, such as drilling, pipe-laying, offloading, and diving support.

The environmental forces acting on a floating vessel are complex and induce at least two distinct kinds of motions. Sea waves consist of a large number of oscillatory components, with several directions, amplitudes and phases. The resulting energy spectrum has a peak value between 0.3 and 1.3 rad/s. Wind-generated waves give rise to large first-order, wave-frequency oscillatory forces, and moments on the vessel. Additionally, environmental loads include slowly varying disturbances caused by wind, current and wave drift forces, which induce low-frequency oscillations, and steady motions on vessels. DPS must suppress or control the low frequency motions, keeping the mean position of the vessel as close as possible to the desired point or track. Wave frequency motions, however, are difficult to be handled by the control system, since they would require an enormous amount of power to be attenuated, leading to extra fuel consumption and increased rate of propellers wear-out, due to thruster modulation (high frequency oscillations in propellers).

Therefore, a sophisticated filtering algorithm must be included in the control loop. The purpose of the wave filter is to separate the wave frequency oscillatory wave induced motion from the motion caused by slowly varying disturbances. Feedback control action must be implemented using the filtered low-frequency vessel motion, enabling thruster modulation and all related problems to be avoided.

Commercial DP systems apply observer based techniques, such as Kalman filtering. One of the main characteristics of Kalman filter is the use of available information regarding the dynamical behavior of the process. The vessel motion due to slow disturbances and due to wave action is modeled. The motion information (predicted by the filter model) is combined with available observations and an optimum state estimator is then constructed. The vessel motion is regarded as the sum of two linearly independent response functions. A low-frequency (LF) model yields motions due to maneuvering forces and environmental forces due to wind, current and wave drift, and a wave-frequency (WF) model yields vessel response due to waves. The idea of separating the filter model into a low and a wave frequency model was originally

Contributed by the Ocean Offshore and Arctic Engineering Division of ASME for publication in the JOURNAL OF OFFSHORE MECHANICS AND ARCTIC ENGINEERING. Manuscript received May 18, 2005; final manuscript received January 4, 2006. Assoc. Editor: John Halkyard. Paper presented at the 24th International Conference on Offshore Mechanics and Arctic Engineering (OMAE2005), June 12, 2005–June 17, 2005, Halkidiki, Greece.

suggested Balchen et al. [1]. Since the model of vessel LF dynamics presents geometrical nonlinearities, the extended Kalman filter (EKF) technique should be used. Furthermore, the WF model depends on an unknown parameter, related to wave frequency. Such parameter is included in the EKF formulation as another state, whose numeric value is continually estimated.

The control algorithm itself calculates thrust forces and moment based on low-frequency motion estimates. Modern commercial systems still employ simple PD algorithms. The integral action is given by the direct compensation of environmental forces, which are also estimated by the Kalman filter, as will be shown in the next section.

The robustness and simplicity of PD controller are the main reasons for its extensive utilization. Furthermore, it meets the performance requirements of a great deal of DP ships. The control parameter tuning procedure is normally carried out during the DPS installation, and sometimes call for execution of some maneuvers in order to assess the ship overall dynamics and maneuverability.

However, during harsh environmental conditions, the control system may display a poor performance, since the PD parameters are usually adjusted under a calm sea state, as described by Bray [2]. Furthermore, in some offshore operations, oil is transferred from one moored FPSO or platform into a DPS shuttle tanker. This operation lasts up to 24 h, and the displacement of the tanker may be increased by a factor of four, altering its dynamic properties. In this case, a constant gain controller is hardly the best approach, given the fact it would require full attention on the part of the tanker operator, who would have to perform manual corrections in the positioning of the tanker, in order to avoid dangerous approximations.

Therefore, fixed-gain PD controller could be inadequate for vessels that must operate under a wide "environmental window" or for ships that present significant displacement variation during the operation. Such and other reasons led the researchers to apply different control methodologies to the DPS. All initiatives feature advantages compared to the constant gain PD, demonstrated by means of experiments or simulations. However, the research community has not been able to convince operators and manufacturers, who still rely on PD controller. Some examples of such novel controllers may be found in [3–5].

In the present paper, the problems associated to the PD controller are solved by means of a robust model-reference adaptive controller. It is shown that the overall structure of the PD controller is still preserved, and that the adaptive algorithm is responsible for the on-line, real-time, correction of control gains. With the present solution, the authors try to address the problem while keeping the simplicity of the PD controller, which is one of the main reasons of its widespread utilization.

The controller is developed and tested in a complete numerical simulator of a shuttle tanker, similar to the vessels operating in Brazilian waters.

System Modeling

The following dynamic model governs the low-frequency horizontal motions of a vessel:

$$(M + M_{11})\ddot{x}_1 - (M + M_{22})\dot{x}_2\dot{x}_6 - M_{26}\dot{x}_6^2 + C_{11}\dot{x}_1 = F_{1E} + F_{1T}$$

$$(M + M_{22})\ddot{x}_2 + M_{26}\ddot{x}_6 + (M + M_{11})\dot{x}_1\dot{x}_6 + C_{22}\dot{x}_2 = F_{2E} + F_{2T} \quad (1)$$

$$(I_Z + M_{66})\ddot{x}_6 + M_{26}\ddot{x}_2 + M_{26}\dot{x}_1\dot{x}_6 + C_{66}\dot{x}_6 = F_{6E} + F_{6T}$$

where I_z is the moment of inertia about the vertical axis; M is the vessel total mass, C_{ij} are damping coefficients, M_{ij} are added mass matrix terms, F_{1E}, F_{2E}, F_{6E} are surge, sway, and yaw environmental loads (current, wind, and waves) and F_{1T}, F_{2T}, F_{6T} are forces and moment delivered by the propulsion system. The variables $\dot{x}_1$, $\dot{x}_2$ are the absolute[1] surge and sway velocities of a central point at midship and $\dot{x}_6$ is the yaw absolute rate of rotation (Fig. 1), all expressed in the ship's moving reference frame.

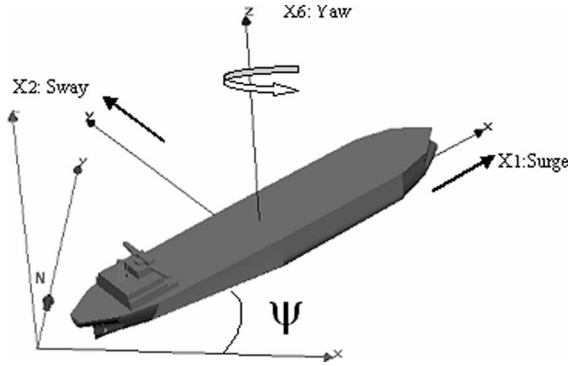

Fig. 1 Coordinate systems

Current induced forces are determined via a heuristic model based on a low aspect ratio wing theory with experimental validation [6]. Wind forces are calculated employing coefficients suggested by OCIMF [7] and wind gusts are also considered. Wave drift forces are evaluated using the hull drift-coefficients worked out by means of a standard second-order potential flow analysis performed by a computer software (Wamit). The interaction between current and waves (wave-drift damping) is also taken into account [8].

Wave-frequency (first-order) motions are evaluated by means of transfer functions related to the wave height, said functions are known as response amplitude operators (RAOs), and are obtained via numerical methods modeling the potential flow around the hull. Such an approach is grounded on the assumption of linear response of wave-frequency motions and on the uncoupling between wave-frequency and low-frequency motions.

Actual sea waves are described by a power spectrum $S(\omega)$ of the free-surface height. The power spectrum of the ship motion i (P_{ii}) is then evaluated by the usual relation

$$P_{ii}(\omega) = \mathrm{RAO}_i(\omega, \beta)^2 \,.\, S(\omega) \quad (2)$$

where β is the wave incidence angle relative to the ship. The wave-frequency motion of the ship is then obtained through a time-serie realization of the power spectrum function P_{ii}.

Extended Kalman Filter Design

As already mentioned, the extended Kalman filter (EKF) technique is broadly used in commercial DPS to perform the tasks of state observation, filtration and others. It must be emphasized, however, that the EKF technique presents several drawbacks. There is a large number of tuning parameters and requires a time-consuming tuning procedure. Furthermore, it requires the use of a gain-scheduling technique, since the model is linearized about approximately 36 yaw angles. As an alternative to the EKF approach, a novel nonlinear observer was recently proposed by Fossen and Strand [9] with excellent results in both simulations and sea-trials. Such observer does not present the problems of EKF, and is based on passivity theory. Nowadays developments indicate that the observer proposed in [9] will soon replace the traditional EKF in modern commercial DPS. However, since the purpose of the present paper is to analyze the controller algorithm, and not the observer itself, the traditional EKF approach will still be adopted.

The extended Kalman filter (EKF) applied to DPS is based on simplified models for LF and WF motions of the vessel. The ap-

[1]With respect to a reference frame fixed to the Earth, Coriolis effects being neglected.

plication was first proposed in [1], with further improvements, results and discussions presented in [10–13]. In the present section such formulation will be briefly adressed.

Under low-speed assumption, the LF motion equation (1) can be simplified, disregarding Coriolis and other second order terms. Therefore, being X and Y the position of the central point of the vessel and ψ_L the (slowly varying) heading angle, the LF dynamics can be described by:

$$\dot{\mathbf{x}}_L = \mathbf{A}_L^{6\times6}\mathbf{x}_L + \mathbf{A}_{EL}^{6\times6}\mathbf{F}_E + \mathbf{E}_L^{6\times3}\boldsymbol{\omega}_L + \mathbf{B}_L^{6\times3}\mathbf{F}_T$$

$$\text{with } \mathbf{A}_L^{6\times6} = \begin{pmatrix} \mathbf{0}_{3\times3} & \mathbf{T}(\psi_L) \\ \mathbf{0}_{3\times3} & -\mathbf{M}^{-1}\mathbf{D}_{3\times3} \end{pmatrix}; \tag{3}$$

$$\mathbf{A}_{EL}^{6\times6} = \mathbf{B}_L^{6\times3} = \mathbf{E}_L^{6\times3} = \begin{pmatrix} \mathbf{0}_{3\times3} \\ \mathbf{M}^{-1} \end{pmatrix};$$

$$\mathbf{T}(\psi_L) = \begin{pmatrix} \cos(\psi_L) & -\sin(\psi_L) & 0 \\ \sin(\psi_L) & \cos(\psi_L) & 0 \\ 0 & 0 & 1 \end{pmatrix}$$

In Eq. (3), $\mathbf{x_L}=(X_L\ Y_L\ \psi_L\ \dot{x}_1\ \dot{x}_2\ \dot{x}_6)^T$, $\mathbf{F_T}$ contains thrusters forces and moment vector, $\mathbf{F_E}$ contains low-frequency environmental forces and moment vector, $\mathbf{M}$ is the mass matrix of vessel, and $\mathbf{D}$ is a damping matrix. The subscript L stands for low-frequency motion. $\boldsymbol{\omega}_L$ is a 3×1 vector containing zero-mean Gaussian white-noise processes with covariance matrix $\mathbf{Q}_L$ ($\boldsymbol{\omega}_L \sim N(0,\mathbf{Q}_L)$)

The forces $\mathbf{F}_E$ are slowly varying unknown variables, and can be modeled by:

$$\dot{\mathbf{F}}_E = \boldsymbol{\omega}_{FL} \tag{4}$$

where ω_{FL} is a 3×1 vector containing zero-mean Gaussian white-noise processes with covariance matrix $\mathbf{Q}_{FL}$ ($\omega_{FL}\sim N(0,\mathbf{Q}_{FL})$).

Finally WF motions can be modeled by [14]:

$$\dot{\mathbf{x}}_H = \mathbf{A}_H^{6\times6}\mathbf{x}_H + \mathbf{E}_H^{6\times3}\boldsymbol{\omega}_H$$

$$\text{with } \mathbf{A}_H^{6\times6} = \begin{pmatrix} \mathbf{0}_{3\times3} & \mathbf{I}_{3\times3} \\ -\omega_0^2\mathbf{I}_{3\times3} & -2\zeta\omega_0\mathbf{I}_{3\times3} \end{pmatrix}; \quad \mathbf{E}_\mathbf{H}^{6\times3} = \begin{pmatrix} \mathbf{0}_{3\times3} \\ \mathbf{I}_{3\times3} \end{pmatrix}; \tag{5}$$

where $\mathbf{x}_H=(\int_0^t X_H d\tau\ \int_0^t Y_H d\tau\ \int_0^t \psi_H d\tau\ X_H\ Y_H\ \psi_H)^T$, $\boldsymbol{\omega}_H$ is a 3×1 vector containing zero-mean Gaussian white-noise processes ($\boldsymbol{\omega}_H\sim N(0,\mathbf{Q}_H)$) and H is used since wave motion are mainly composed by high-frequency components. The parameter ζ is the nondimensional damping ratio of the motions, and was set as 0.1.

The parameter ω_0 represents the peak frequency of the motion power spectrum, which is close together to the peak frequency of the wave spectrum. Such parameter undergoes on-line estimation, since its numerical value is unknown and the environmental conditions may vary during the operation. It is a common practice in commercial DPS to introduce such parameter as a new state in the Kalman filter model. Being a slowly varying parameter, its dynamics is given by:

$$\dot{\omega}_0 = \omega_\omega \tag{6}$$

where ω_ω is a zero-mean Gaussian white-noise process ($\omega_\omega \sim N(0,Q_\omega)$).

The measured signals $\mathbf{z}$ are given by:

$$\mathbf{z} = \begin{pmatrix} X_L + X_H + v_X \\ Y_L + Y_H + v_Y \\ \psi_L + \psi_H + v_\psi \end{pmatrix} \tag{7}$$

where $\mathbf{v}$ is a 3×1 vector containing zero-mean, Gaussian white noise processes ($\mathbf{v}\sim N(0,\mathbf{R})$).

For the sake of simplicity, the matrixes $\mathbf{Q}_L$, $\mathbf{Q}_H$, $\mathbf{Q}_{FL}$, and $\mathbf{R}$ are considered diagonal in real applications.

It should be emphasized that the EKF estimates the components $\mathbf{x}_H$ and $\mathbf{x}_L$ and also low-frequency environmental forces $\mathbf{F}_E$.

The complete model can be written as:

$$\dot{\mathbf{x}} = \mathbf{A}(\mathbf{x})\ .\ \mathbf{x} + \mathbf{B}\mathbf{F}_T + \mathbf{E}\boldsymbol{\omega}$$

$$\mathbf{z} = \mathbf{H}\mathbf{x} + \mathbf{v} \tag{8}$$

with:

$$\mathbf{x} = \begin{pmatrix} \mathbf{x}_L \\ \mathbf{x}_H \\ \mathbf{F}_{EL} \\ \omega_0 \end{pmatrix};\ \boldsymbol{\omega} = \begin{pmatrix} \boldsymbol{\omega}_L \\ \boldsymbol{\omega}_H \\ \boldsymbol{\omega}_{F_{EL}} \\ \omega_\omega \end{pmatrix};\ \mathbf{B} = \begin{pmatrix} \mathbf{B}_L^{6\times3} \\ \mathbf{0}^{6\times3} \\ \mathbf{0}^{4\times3} \end{pmatrix};$$

$$\mathbf{A}(\mathbf{x}) = \begin{pmatrix} \mathbf{A}_L^{6\times6}(\mathbf{x}) & \mathbf{0}^{6\times6} & \mathbf{A}_{EL}^{6\times3} & \mathbf{0}^{6\times1} \\ \mathbf{0}^{6\times6} & \mathbf{A}_H^{6\times6}(\mathbf{x}) & \mathbf{0}^{6\times3} & \mathbf{0}^{6\times1} \\ \mathbf{0}^{4\times6} & \mathbf{0}^{4\times6} & \mathbf{0}^{4\times3} & \mathbf{0}^{4\times1} \end{pmatrix};$$

$$\mathbf{E} = \begin{pmatrix} \mathbf{E}_L^{6\times3} & \mathbf{0}^{6\times3} & \mathbf{0}^{6\times4} \\ \mathbf{0}^{6\times3} & \mathbf{E}_H^{6\times3} & \mathbf{0}^{6\times4} \\ \mathbf{0}^{4\times3} & \mathbf{0}^{4\times3} & \mathbf{I}^{4\times4} \end{pmatrix};\ \mathbf{H} = (\mathbf{I}^{3\times3}\ \mathbf{0}^{3\times3}\ \mathbf{0}^{3\times3}\ \mathbf{I}^{3\times3}\ \mathbf{0}^{3\times4})$$

The following discrete version of Eq. (8) is used in the extended Kalman filter algorithm, being Δt the sampling time:

$$\mathbf{x}[k] = \mathbf{f}(\mathbf{x}[k-1],\mathbf{F_T}[k-1],\boldsymbol{\omega}[k-1])$$

$$\mathbf{z}[k] = \mathbf{H}\ .\ \mathbf{x}[k] + \mathbf{v}[k] \tag{9}$$

$$\mathbf{f}(.,.,.) = (\mathbf{A}(\mathbf{x})\ .\ \Delta t + \mathbf{I})\ .\ \mathbf{x}[k-1] + \mathbf{B}\ .\ \Delta t\ .\ \mathbf{F_T}[k-1] + \mathbf{E}\ .\ \Delta t\ .\ \boldsymbol{\omega}[k-1]$$

Being $\bar{\mathbf{x}}$ and $\hat{\mathbf{x}}$ the a priori and the a posteriori estimates of the state vector, $\mathbf{X}$ the error matrix covariance, and $\mathbf{K}$ the Kalman gain matrix, the discrete EKF is given by [15]:

Prediction

$$\bar{\mathbf{x}}[k+1] = \mathbf{f}(\hat{\mathbf{x}}[k],\mathbf{F_T}[k],0)$$

$$\bar{\mathbf{X}}[k+1] = \boldsymbol{\Phi}\ .\ \hat{\mathbf{X}}[k]\ .\ \boldsymbol{\Phi}^T + \boldsymbol{\Gamma}\ .\ \mathbf{Q}\ .\ \boldsymbol{\Gamma}^T$$

$$\text{with } \boldsymbol{\Phi} = \partial\mathbf{f}/\partial\mathbf{x}\big|_{\mathbf{x}=\hat{\mathbf{x}}[k]};\ \boldsymbol{\Gamma} = \mathbf{E}\ .\ \Delta t \text{ and } \mathbf{Q} = \begin{pmatrix} Q_L & 0 & 0 & 0 \\ 0 & Q_H & 0 & 0 \\ 0 & 0 & Q_{FL} & 0 \\ 0 & 0 & 0 & Q_\omega \end{pmatrix} \tag{10a}$$

Correction

$$\mathbf{K}[k] = \bar{\mathbf{X}}[k]\ .\ \mathbf{H}^T\ .\ (\mathbf{H}\ .\ \bar{\mathbf{X}}[k]\ .\ \mathbf{H}^T + \mathbf{R})^{-1}$$

$$\hat{\mathbf{x}}[k] = \bar{\mathbf{x}}[k] + \mathbf{K}[k]\ .\ (z[k] - \mathbf{H}\ .\ \bar{\mathbf{x}}[k]) \tag{10b}$$

$$\hat{\mathbf{X}}[k] = (I - \mathbf{K}[k]\ .\ \mathbf{H})\ .\ \bar{\mathbf{X}}[k]$$

Figure 2 presents a block diagram featuring the EKF and the controller, which will be analyzed in the next section. It must be recalled that DP systems usually contain a feed forward loop to compensate for wind effects. Wind speed and direction are measured by anemometers, and the forces are evaluated using the wind coefficients of the ship. Such forces are directly compensated by the controller and counteracted before causing a positioning error. These estimates are also used by the Kalman filter, which must subtract them from the total thrust forces, resulting in the parcel of thrust responsible for current and wave compensation.

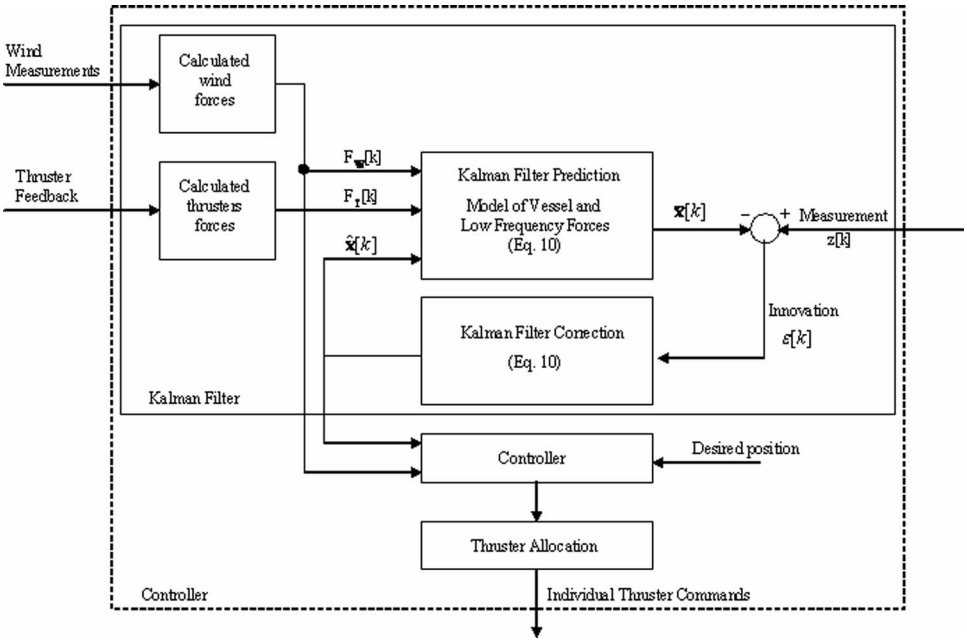

Fig. 2 Kalman filter and controller block diagram

Robust Model-Reference Adaptive Control

The Model-Reference Adaptive Control Algorithm. Adaptive control laws operating on the model-reference concept are usually designed in such way that the plant under consideration should display a dynamic behavior that matches that of a dynamic system known as reference model. Hence the name model-reference adaptive controller (MRAC) with which said control algorithm was coined.

The concept of MRAC was firstly proposed in [16], and several applications and improvements were developed since then (for, e.g., [17–19]). Here, though, we shall present an abridged version of MRAC that suits the problem at hand, while retaining the original structure originally proposed. For simplicity, we will restrict ourselves to presenting the derivation of the controller for just one-degree of freedom. The complete design actually considers three independent controllers, one for each degree of freedom.

Equation (11) represents the dynamic behavior exhibited by the reference model:

$$M_m\ddot{y}_m + B_m\dot{y}_m + K_m y_m = u_c(t) \tag{11}$$

The plant dynamics is given in Eq. (12):

$$M\ddot{y} + B\dot{y} = u(t) \tag{12}$$

We shall now introduce $z(t)$:

$$z(t) = \ddot{y}_m - \beta_1\dot{e} - \beta_0 e \tag{13}$$

where $e=y-y_m$. It follows from this definition that e is expected to converge asymptotically to zero (the plant should match the reference model). Now, let us define the vector $\mathbf{v}=[z(t)\dot{y}]^T$ and the vector of estimated parameters $\hat{\mathbf{a}}(\mathbf{t})=[\hat{a}_2\hat{a}_1]^T$. We have then laid the basis to define the control law, which is given by:

$$u(t) = \hat{a}_2 z(t) + \hat{a}_1\dot{y} \tag{14}$$

At this point, all that is left is to evaluate the law for the adaptation mechanism. The error $(e=y-y_m)$ dynamics can be written as:

$$\ddot{e} + \beta_1\dot{e} + \beta_0 e = (1/a_2)\mathbf{v^T}(t)\,.\,\tilde{\mathbf{a}}(t) \tag{15}$$

where β_0 and β_1 are positive constants such that $s^2+\beta_1 s+\beta_0$ is a stable (Hurwitz) polynomial and $\tilde{\mathbf{a}}(t)=\hat{\mathbf{a}}(t)-\mathbf{a}(t)$. Equation (15) can be rewritten in the state-space form as:

$$\dot{\mathbf{x}} = \mathbf{A}\mathbf{x} + \mathbf{b}[(1/a_2)\mathbf{v^T}\tilde{\mathbf{a}}]$$

$$\text{with } \mathbf{A} = \begin{pmatrix} 0 & 1 \\ -\beta_0 & -\beta_1 \end{pmatrix};\ \mathbf{b} = \begin{pmatrix} 0 \\ 1 \end{pmatrix};\ \mathbf{x} = \begin{pmatrix} e \\ \dot{e} \end{pmatrix}. \tag{16}$$

Introducing the matrices Γ, $\mathbf{P}$, and $\mathbf{Q_C}$, being $\mathbf{\Gamma}$ and $\mathbf{P}$ symmetric positive definite constant matrices, $\mathbf{PA}+\mathbf{A^TP}=-\mathbf{Q_C}$, $\mathbf{Q_C}=\mathbf{Q_C^T}$, with $\det(\mathbf{Q_c})>0$. The adaptation law is then given by:

$$(\dot{\hat{a}}_2\ \dot{\hat{a}}_1)^T = -\,\mathbf{\Gamma}\,.\,\mathbf{v}\,.\,\mathbf{b}^T\,.\,\mathbf{P}\,.\,\mathbf{x} \tag{17}$$

It is possible to show the convergence of $\mathbf{x}$ using Barbalat's Lemma. Therefore, with the adaptive controller defined by both the adaptation and the control law, $\mathbf{x}$ converges to zero. The condition for parameter convergence can be shown to be the *persistent excitation* of the vector $\mathbf{v}$.

Using $\beta_0=K_m/M_m$ and $\beta_1=B_m/M_m$, the polynomial $s^2+\beta_1^s+\beta_0$ will clearly represent a stable system. Substituting Eq. (14) into Eq. (12), the following closed-loop dynamics is obtained:

$$M\ddot{y} + B\dot{y} = \hat{a}_2 z(t) + \hat{a}_1\dot{y} \tag{18}$$

Using Eqs. (11) and (13), Eq. (18) can be written as:

$$M\ddot{y} + B\dot{y} = \hat{a}_2\left(\frac{u_c(t)}{M_m} - \beta_1\dot{y} - \beta_0 y\right) + \hat{a}_1\dot{y}$$

$$\frac{M\,.\,M_m}{\hat{a}_2}\ddot{y} + \frac{.M_m}{\hat{a}_2}(B + \hat{a}_2\beta_1 - \hat{a}_1)\dot{y} + \hat{a}_2\beta_0 y = u_c(t) \tag{19}$$

Since the tracking error converges to zero, Eq. (19) converges to the reference model Eq. (11), which is only made possible if $\hat{a}_2\rightarrow M$ and $\hat{a}_1\rightarrow B$.

The analogy between a PD controller and the previously derived MRAC is obtained by means of Eq. (14), that can also be written as:

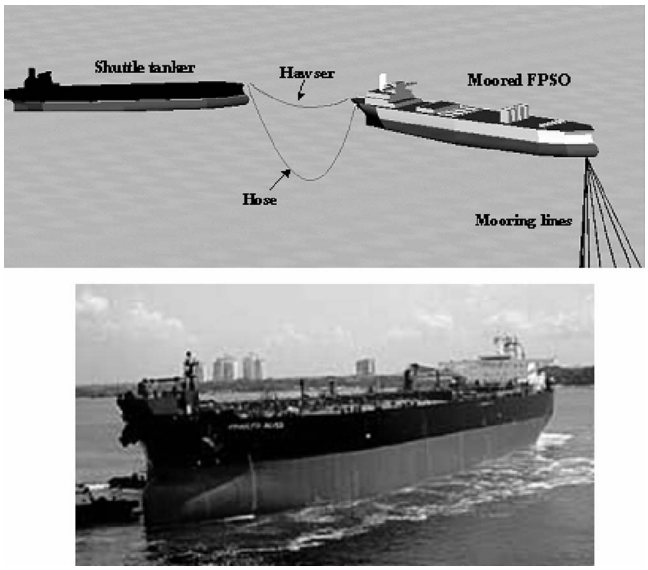

Fig. 3 (Up) Offloading operation; (down) picture of shuttle tanker in ballasted condition

$$u(t) = -\hat{a}_2\beta_1\dot{e} + \hat{a}_1\dot{y} - \hat{a}_2\beta_0 e + \hat{a}_2\ddot{y}_m$$

where the first and second terms are responsible for the derivative action and the third term gives the proportional action. For the surge motion, in which the damping factor B is extremely small ($B \ll B_m$), the equivalent constant P and D gains are given by:

$$P = -\hat{a}_2\beta_0 = -M \cdot \frac{K_M}{M_M};\ D = -\hat{a}_2\beta_1 = -M \cdot \frac{B_M}{M_M} \qquad (20)$$

The Robust Model-Reference Adaptive Control Algorithm. In the early 80s, relatively simple examples were employed to show that adaptive schemes designed to perform under disturbance-free conditions could actually become unstable, should external disturbances be added to the system. Such examples led engineers back then to claim that current adaptive schemes failed to display robust properties relative to external disturbances.

Those conclusions spawned a wave of research efforts to "robustify" the existing algorithms, so that external disturbances could be rejected.

In the dynamic positioning scenario, environmental loads are viewed as external disturbances by the control system. We shall now modify the control law in (14) by adding an extra term. The resulting control law will then feature robust properties relative to the presence of environmental forces.

The modified control law is given by [20,21]:

$$u(t) = v^T(t) \cdot \hat{a}(t) - R \cdot sat(e)$$
$$\text{where } \mathrm{sat}(e) = \begin{cases} e & |e| \leq \phi \\ \phi & |e| > \phi \end{cases} \qquad (21)$$

ϕ being the thickness of the boundary layer. The gain R is such that $|d(t)| \leq R$, that is, the upper bound of the disturbance magnitude.

The control law in (21) can be shown to be globally stable, in the sense of boundness. Furthermore, it can be shown that $e(t)$ will converge to zero [20].

Case Study

The controller was implemented in a numerical simulator, considering a real shuttle vessel operating in Brazilian waters during an offloading operation (Fig. 3). The main properties of the tanker in both, ballasted and loaded conditions are presented in Table 1.

Table 1 Tanker main properties

Property	Full load condition	Ballasted condition
Length (L)	260 m	
Beam (B)	44.5 m	
Draft (T)	16.1 m	6. 4 m
Mass	156,310 ton	58,783 ton
Yaw Inertia	6.6×10^8 ton.m^2	2.5×10^8 ton.m^2
Added Mass (M_{11})[a]	8,510 ton	1,560 ton
Added Mass (M_{22})[a]	142,000 ton	24,100 ton
Added Mass (M_{66})[a]	9.7×10^8 ton.m^2	0.9×10^8 ton.m^2

[a]Low frequency

The simulation reproduces the first 5 h out of a 12 h long operation, throughout which the tanks of the ballasted ship are loaded up with oil getting transferred in from the FPSO. The shuttle tanker is kept lined up with the FPSO, at a distance of approximately 100 m. Therefore, position and heading control is critical, due to the risk of collision as well as hose rupture. So, the FPSO position must be monitored and, in case of large amplitude motions, the DPS must relocate the shuttle, which must be kept at a safe distance away from the FPSO. In order to assess the controller performance, corrections of 20 m every 30 min in surge, 10 m every 20 min in sway and 20 deg every 33 min in yaw, were considered. The simulation attempts to reproduce the actual control strategy employed in commercial DPS set up in shuttle vessels. As a fuel-saving procedure, the shuttle tanker does not follow all motions of the FPSO, being relocated only when the FPSO displays a pronounced displacement [22]. Figure 4 shows the en-

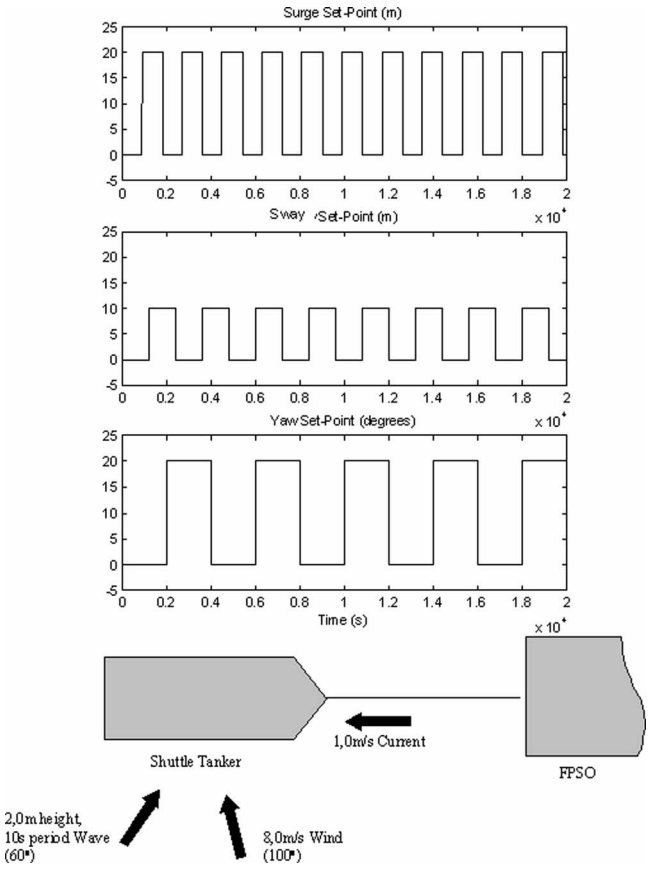

Fig. 4 (Up) Set-points; (down) environmental conditions

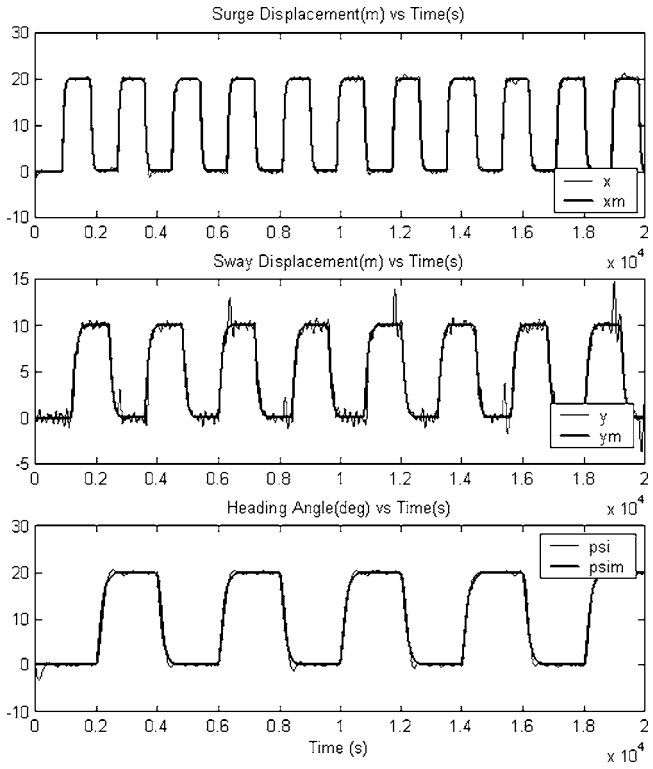

Fig. 5 Actual positions and heading compared to reference model (subscript$_m$) outputs

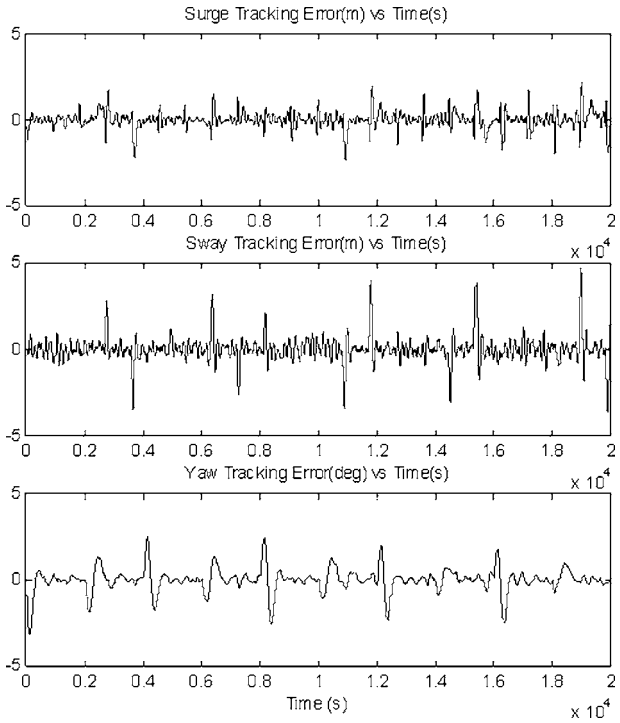

Fig. 6 Tracking errors $e=y-y_m$

vironmental conditions and set-points considered in the simulations.

Main control and filter parameters are given by:

$$\mathbf{Q} = \text{diag}(4\times10^{10}\ 4\times10^{10}\ 4\times10^{14}\ 3.4\ 3.4\ 0.02\ 3\times10^{10}\ 3\times10^{10}\ 3\times10^{14}\ 5\times10^{-5})$$

$$\mathbf{R} = \text{diag}(1\ 1\ 3\times10^{-4})$$

$$\mathbf{\Gamma}_x = \text{diag}(2.2\times10^{9}\ 5\times10^{5}) \quad \mathbf{Q_{Cx}} = \mathbf{I}_{2\times2}\times6.5\times10^{-6}$$

$$\mathbf{\Gamma}_y = \text{diag}(3.8\times10^{9}\ 1.6\times10^{7}); \quad \mathbf{Q_{Cy}} = \mathbf{I}_{2\times2}\times7.5\times10^{-6}$$

$$\mathbf{\Gamma}_z = \text{diag}(3.9\times10^{15}\ 4.4\times10^{9}) \quad \mathbf{Q_{Cz}} = \mathbf{I}_{2\times2}\times6.5\times10^{-5}$$

Figure 5 shows the simulation results, considering the adaptive control. The reference model is made up of three uncoupled and critically damped second-order systems, with natural periods of 200 s for surge, 400 s for sway, and 600 s for yaw motion. The reference-model is tracked with good accuracy, despite the displacement variation, with virtually no performance loss. After a short transient, the tracking error $e=y-y_m$ is reduced to values smaller than 2.5 m for surge, 5 m for sway and 3 deg for yaw, as it is shown in Fig. 6. Figure 7 presents control forces and moment, the magnitudes of which show the tendency to escalate as the simulation goes on, due to the increase of mass and due to damping, wave, and current forces.

The adaptive controller estimation for the mass matrixes is shown in Fig. 8. The differences between actual values and predicted ones are actually bounded, as predicted by theory.

A paramount condition for a convergent parameter estimation in adaptive controllers is the presence of a persistent excitation. Observe Fig. 8 and notice that in the sway direction, the estimation process performs quite well indeed, while in the surge direction—where the environmental loads are a lot less pronounced as far as their magnitude are concerned—the mass estimation process follows a very similar trend to that of the actual vessel mass, only it is shifted downwards. The increase in the estimated mass over time mirrors what goes on as the offloading operation is carried out, namely the shuttle tanker undergoes an increase in its inertia.

The constant-gain PD controller was also applied to the problem. The simulation result is presented in Fig. 9. The performance loss during the offloading operation becomes evident, as the ship's

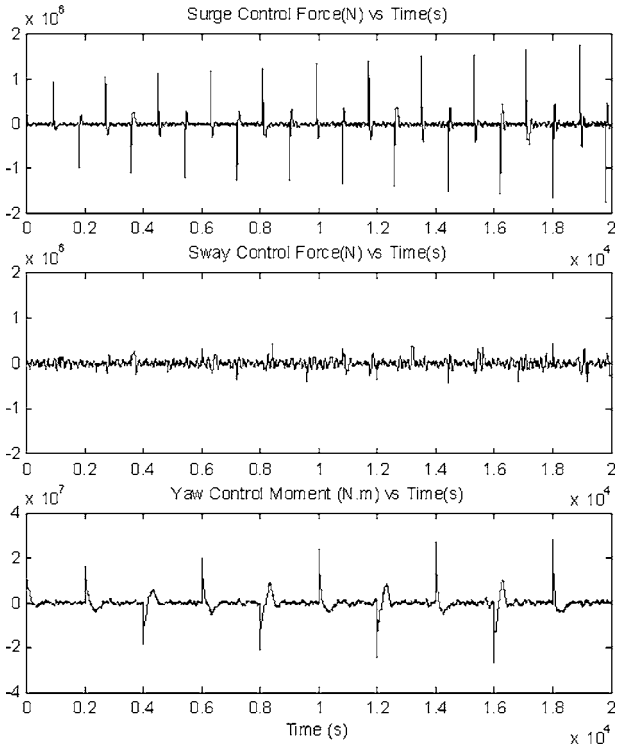

Fig. 7 Control forces and moment

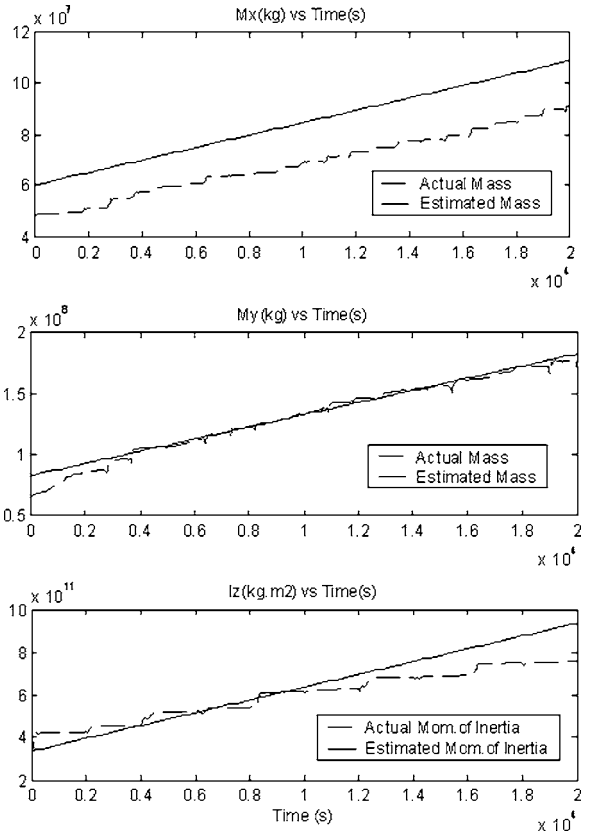

Fig. 8 Surge, sway, and yaw, mass matrix estimation

mass and main dynamic properties undergo a substantial variation. Since the P and D parameters of the controller were evaluated by Eq. (20) considering the ballasted mass of the ship, the performance of the controller is better in the beginning of the operation,

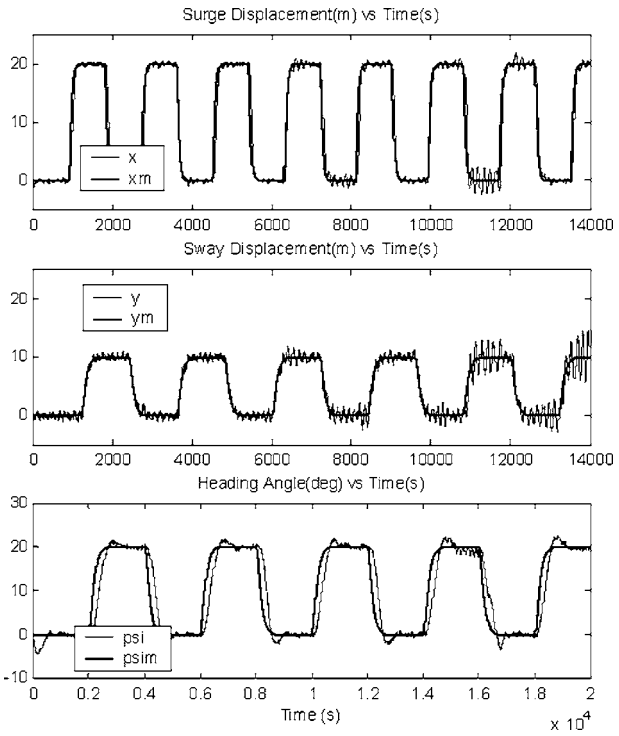

Fig. 9 Actual positions and heading and set-tracks

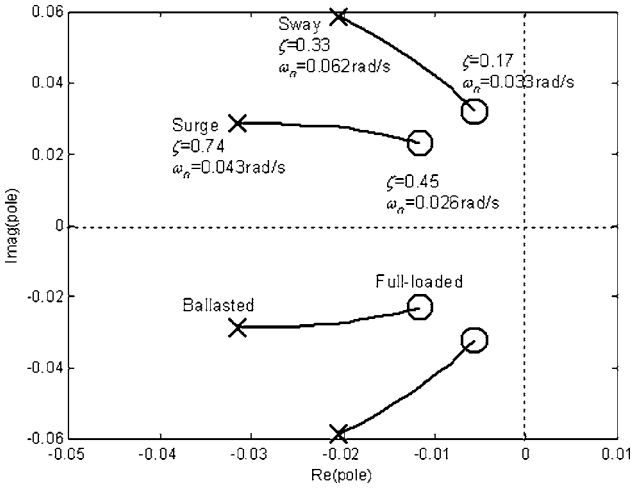

Fig. 10 Root-locus for sway and surge motions, considering the variation of mass during offloading operation

getting worse as the inertia increases. The overshoot of the closed loop response increases, what may cause dangerous approximation between the ships.

A simple analysis shows that a constant-gain controller may lead to oscillatory behavior as the mass increases. In fact, disregarding the coupling between sway and yaw, the following equation represents the closed-loop transfer function of each motion:

$$\frac{D_i s + P_i}{(M + M_{ii})s^2 + (D_i + C_{ii})s + P_i} \tag{22}$$

where P_i and D_i are the proportional and derivative gains of the controller in the direction i (i=1, 2, or 6). The correspondent damping (ζ_i) and natural frequency (ω_{ni}) are given by:

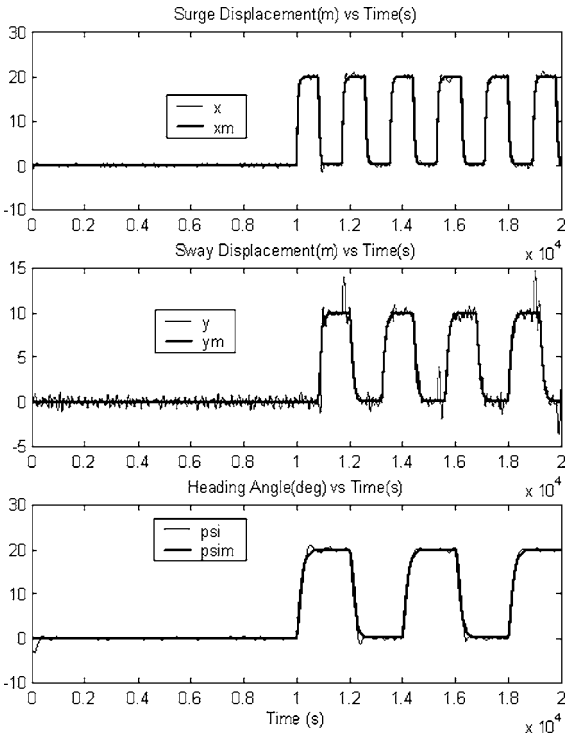

Fig. 11 Reference model response and vessel response (simulation 2)

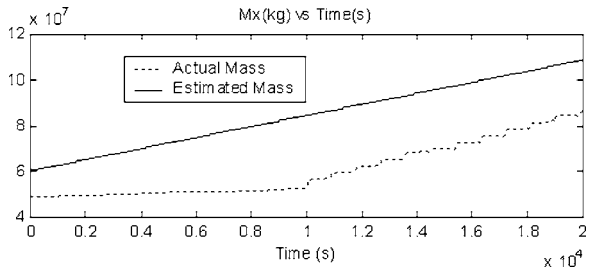

Fig. 12 Surge mass estimation

$$\omega_{ni} = \sqrt{\frac{P_i}{M + M_{ii}}};\ \zeta_i = \frac{D_i + C_{ii}}{2\sqrt{P_i \,.\, (M + M_{ii})}} \tag{23}$$

As expected, for an increasing mass, the damping coefficient decreases, and the closed loop system is equivalent to a subcritically damped oscillator. Furthermore, the natural frequency of the oscillator also decreases. Figure 10 presents the root-locus of sway and surge closed-loop dynamics. In the beginning of the operation, the surge equivalent damping factor, for example, is approximately 0.74, and decreases to 0.45 in the final phase of the operation. That would explain the rather pronounced oscillatory behavior observed during the simulation (Fig. 9), which only goes to show one of the drawbacks of applying a constant gain controller to the present operation

As an additional test, in order to evaluate MRAC performance with a nonpersistent excitation, a different simulation was carried out. During the first 10,000, the ship position and heading is kept constant. The corrections in the set-point are initiated at this instant. Figure 11 shows that the performance of the system is good, with a small tracking error for the three degrees of freedom. Of course, the mass (inertia) estimation is affected by the nonpersistent excitation in the first part of the operation, as shown in Fig. 12 for surge total mass. However, the parameter error is bounded, and does not affect the overall tracking performance.

Conclusions

This work presented the application of a robust model-reference adaptive control technique to DPSs, cascaded with the commonly used extended Kalman filter. The controller was applied to a dynamic positioned shuttle tanker subjected to waves and current, during the offloading operation. The simulation results showed that a good performance is kept during all the operation, despite the significant variations in dynamic properties of the vessel arising from the oil transfer process. If a persistent excitation is present, the adaptive algorithm was able to estimate the mass of the vessel with a good accuracy. However, even without such excitation, the adaptive law was able to adjust the controller correctly, keeping a good tracking performance in spite of a poor parameter estimation.

For the sake of comparison, a fixed-gain PD controller was also applied, and it was shown that such controller is not able to cope with substantial variations in dynamic properties of the vessel, consequently, a loss in performance was observed as the offloading operation proceeded.

Based on a wide range of numerical simulation results, all it could be observed, up to this point, is that the cascaded system made up of a Kalman filter and Robust MRAC has never shown any evidence whatsoever of what could go under the heading of unstable behavior. The KF equations are based on the assumption of a linearized ship model, therefore, the KF algorithm can be shown to be locally stable as long as the linear assumption holds. As for the R-MRAC, [20] shows that the proposed algorithm is actually globally assimptotically stable (GAS). When we, then, proceed to set up the R-MRAC with the KF equations, the resulting cascaded system must be analyzed. In fact, the lingering question "Do we have global stability for the resulting cascaded system?" has steered a new research effort on our part whose main purpose boils down to providing a formal mathematical proof to show that the resulting cascaded system would be actually globally stable. For example, Loria et al. [23] presented a separation principle for dynamic positioning of ships which can be applied to a cascaded observer-controller system. Such reference, among others, will be used as a starting point of the stability analysis we shall be conducting further.

Acknowledgment

This work has been supported by Petrobras and the State of São Paulo Research Foundation (FAPESP—Process no. 03/12330-3 and 02/07946-2). A CNPq research grant, process No. 302450/2002-5, is also acknowledged. The authors gratefully acknowledge the valuable contributions of the reviewers.

References

[1] Balchen, J. G., Jenssen, N. A., and Saelid, S., 1976, "Dynamic Positioning Using Kalman Filtering and Optimal Control Theory," *Proceedings of IFAC/IFIP Symposium on Automation in Offshore Oil Field Operation*, Bergen.

[2] Bray, D., 1998, *Dynamic Positioning*, The Oilfield Seamanship Series, Volume 9, Oilfield Publications Ltd., (OPL).

[3] Katebi, M. R., Grimble, M. J., and Zhang, Y., 1997, "H_∞ Robust Control Design for Dynamic Ship Positioning," IEE Proc.: Control Theory Appl., **144**(2), pp. 110–120.

[4] Aarset, M. F., Strand, J. P., and Fossen, T. I., 1998, "Nonlinear Vectorial Observer Backstepping With Integral Action and Wave Filtering for Ships," *Proceedings of the IFAC Conference on Control Applications in Marine Systems* (CAMS'98), Fukuoka, Japan, pp. 83–89.

[5] Tannuri, E. A., Donha, D. C., and Pesce, C. P., 2001, "Dynamic Positioning of a Turret Moored FPSO Using Sliding Mode Control," Sitzungsber. Akad. Wiss. Wien, Math.-Naturwiss. Kl., Abt. 2A, **11**, pp. 1239–1256.

[6] Simos, A. N., Tannuri, E. A., Pesce, C. P., and Aranha, J. A. P., 2001, "A Quasi-Explicit Hydrodynamic Model for the Dynamic Analysis of a Moored FPSO Under Current Action," J. Ship Res., **45**(4), pp. 289–301.

[7] OCIMF, 1994, "Predictions of Wind and Current Loads on VLCCs," Oil Companies International Marine Forum.

[8] Aranha, J. A. P., 1994, "A Formula for Wave Damping in the Drift of a Floating Body," J. Fluid Mech., **272**, pp. 147–155.

[9] Fossen, T. I., and Strand, J. P., 1999, "Passive Nonlinear Observer Design Using Lyapunov Methods, Experimental Results With a Supply Vessel," Automatica, **35**(1), pp. 3–16.

[10] Saelid, S., Jenssen, N. A., and Balchen, J. G., 1983, "Design and Analysis of a Dynamic Positioning System Based on Kalman Filter and Optimal Control," IEEE Trans. Autom. Control, **AC-28**(3), pp. 331–339.

[11] Fung, P. T. K., and Grimble, M. J., 1983, "Dynamic Positioning Using a Self-Tuning Kalman Filter," IEEE Trans. Autom. Control, **AC-28**(3), pp. 339–350.

[12] Di Masi, G. B., Finesso, L., and Picci, G., 1986, "Design of a LQG Controller for Single Point Moored Large," Automatica, **22**(2), pp. 155–169.

[13] Tannuri, E. A., Bravin, T. T., and Pesce, C. P., 2003, "Dynamic Positioning Systems: Comparison Between Wave Filtering Algorithms and Their Influence on Performance," *Proceedings OMAE2003 Conference*, June 3–13, Cancun, Mexico.

[14] Balchen, J. G. et al., 1980, "A Dynamic Positioning System Based on Kalman Filtering and Optimal Control," Modeling, Identification and Control, **1**(3), pp. 135–163.

[15] Cadet, O., 2003, "Introduction to Kalman Filter and its use in Dynamic Positioning Systems," *Proceedings of Dynamic Positioning Conference*, September 16–17, Houston, USA.

[16] Whitaker, H. P., Yamron, J., and Kezer, A., 1958, "Design of Model Reference Adaptive Control Systems for Aircraft," Report R-164, Instrumentation Laboratory, M. I. T. Press, Cambridge, Massachusetts.

[17] Narendra, K. S., and Annaswamy, A. M., 1989, *Stable Adaptive Systems*, Prentice Hall, Englewood Cliffs, New Jersey.

[18] Ioannou, P. A., and Sun, J., 1996, *Robust Adaptive Control*, Prentice Hall, Englewood Cliffs, N.J.

[19] Slotine, J. J. E., and Li, W., 1991, *Applied Nonlinear Control*, Prentice Hall, Englewood Cliffs, N.J.

[20] Feng, G., 1994, "New Robust Model Reference Adaptive Control Algorithm," Child Today, **141**(3), pp. 177–180.

[21] Slotine, J. E., and Sastry, S., 1983, "Tracking Control of Nonlinear Systems Using Sliding Surfaces With Applications to Robot Manipulators," Int. J. Control, **38**, pp. 465–492.

[22] Bravin, T. T., and Tannuri, E. A., 2004, "Dynamic Positioning Systems Applied to Offloading Operations," International Journal of Maritime Engineering (IJME), **146**, 1–18.

[23] Loria, A., Fossen, T. I., and Panteley, E., 2000, "A Separation Principle for Dynamic Positioning of Ships: Theoretical and Experimental Results," IEEE Trans. Control Syst. Technol., **TCST-8**(2), pp. 332–343.